An enhanced distributed acoustic sensing system based on the interactions between microstructures

An enhanced distributed acoustic sensing system based on the interactions between microstructures

X P Zhang[1, 2], Y Y Shan[1], Y H Zhang[1], J Reng[1], M M Chen[3, 4]*, Y X Zhang[1, 2]*

[1] Institute of Optical Communication Engineering, Nanjing University, China
[2] Key Laboratory of Modern Acoustics, Nanjing University, China
[3] School of Electronics and Engineering, Nanjing Xiaozhuang University, China
[4] Optoelectronics Research Centre, University of Southampton, UK

E-mail: chenmm@njxzc.edu.cn; zyixin@nju.edu.cn

Abstract. Acoustic field could be quite useful in structure health monitoring (SHM). Here we present an enhanced distributed acoustic sensing (DAS) system by implanting microstructures into the sensing fibre. Taking advantage of the interactions between nearby microstructures, the acoustic field could be reconstructed with high fidelity and signal-to-noise ratio (SNR) even at the rear end of 42.2km long sensing fibre. The experimental results have shown that the proposed sensing system has a linear intensity response of R^2=0.9988, while its frequency response band ranges from 8Hz to 1 kHz. Purely distributed sensing along the optical fibre has been obtained even with discretely implanted microstructures for the proposed system, which offers a dependable option for acoustic field monitoring.

1. Introduction

High accuracy monitoring of acoustic field could be quite useful in structure health monitoring (SHM) [1-3]. Recently the distributed acoustic sensing (DAS) system has attracted a significant amount of research attention, owing to its outstanding advantages of long sensing range, high sensitivity, fast response, accurate location, immunity to electromagnetic interference and fully distributed sensing ability [4-8].

Valuable work has been made to improve the performance of DAS. Juarez utilized a continuous-wave Er3+ doped fibre Fabry-Perot laser and an electro-optic modulator to improve the sensing range to 12km[4]. The erbium-doped fibre amplifier (EDFA) can significantly boost the input power launched into the sensing fibre[9, 10], but the sensing range of EDFA-based DOFS would be limited by rapidly accumulated nonlinear effects along the fibre[11], which severely degrades the coherence of the probe signal. Then the distributed optical fibre amplifier based on Raman or Brillouin pump was applied in DOFS[12-15] to gain the probe light along the entire sensing fibre, and the sensing range could be improved up to 175km[12]. However, the complexity of the sensing system is increased which may lead to the degradation of flexibility in practical applications. To further improve the signal-to-noise ratio (SNR), microstructures have been induced to the sensing fibre. C. Wang *et al*. combined ultra-weak fibre Bragg gating (UWFBG) with phase-sensitive optical time domain reflectometry (Φ-OTDR) for acoustic measurement and achieved a sensitivity of -158dB[16]. F. Zhu *et al.* embedded UWFBG array at the end of sensing fibre and $\mu\varepsilon$ level dynamic strain has been captured[17]. X. C. Wang *et al*. have proposed an enhanced polarization optical time domain reflectometry (P-OTDR) for vibration monitoring based on UWFBG. The SNR of system was improved by 11dB[18]. However, the microstructures in these cases just acted as a substitution for the Rayleigh scattering points within the sensing fibre to provide higher and more stable reflectivity.

In this paper, we proposed a new DAS scheme based on self-heterodyne detection. Taking advantage of the interaction between nearby microstructures, the acoustic field could be fully reconstructed with high fidelity and SNR without the help of additional demodulation structure.

2. Principle and Experimental Setup

Fig.1(a) presents the experimental setup of the proposed system. A 1550.12nm narrow linewidth laser (RIO Orion Laser Module) was selected as the light source, whose linewidth was 3.7kHz. The continuous-wave (CW) of laser was separated into two paths by an optical coupler (OC_1). Then the CW waves were shaped by two acoustic optical modulators ($AOM_{1,2}$) into narrow probe pulses with frequency shift of 150MHz and 80MHz. The repetition period and width of the probe pulses

were 500μs and 80ns, respectively. There was a time delay τ=100ns between these two pulses. The two pulses were combined by OC_2 and amplified by an EDFA. Optical filter was inserted to minimize the amplifier spontaneous emission (ASE). The probe pulses passed through a circulator (Cir) and launched into the sensing fibre through 1550nm port of the wavelength division multiplexer (WDM).

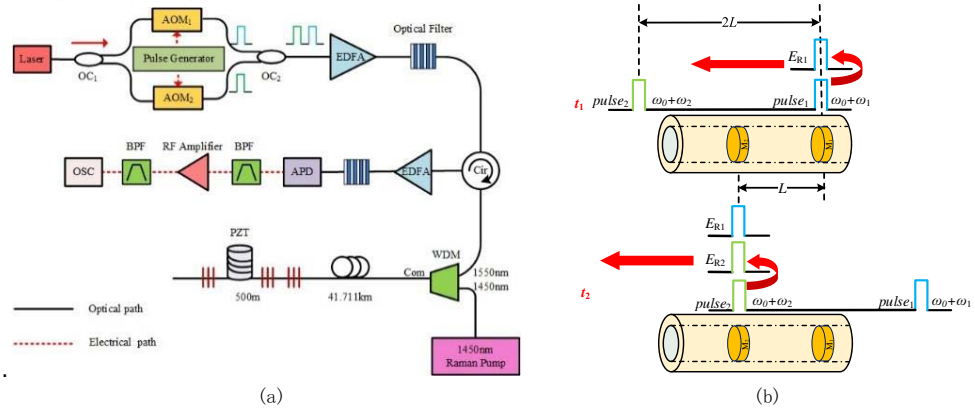

(a) (b)

Fig.1 (a)Experimental setup of proposed system. $OC_{1,2}$: optical coupler; $AOM_{1,2}$: acoustic-optic modulator; EDFA: erbium-doped fibre amplifier; Cir: circulator; WDM: wavelength division multiplexer; APD: avalanche photodiode; BPF: band pass filter; OSC: oscilloscope. (b)Principle of interaction process between microstructures and self-heterodyne detection

More than fifty microstructures were implanted at the end of 41.711km sensing fibre as wideband weak reflection surfaces, generating reflected light waves that were much stronger than Rayleigh back-scattering (RBS). The Raman pump was a Raman Fibre Laser (KEOPSYS) emitting at 1450nm with the maximum output power of 5W. The reflected light waves back from the sensing fibre first went through a small-signal-EDFA and another optical filter, and then received by a 200MHz avalanche photodiodes (APD). The output of APD passed through two electrical band pass filters (BPF) and a RF amplifier for signal conditioning. The output of the second BPF was recorded by oscilloscope (OSC) with a sampling rate of 1GSa/s that was in synchronization with the AOM by the pulse generator. PZT wrapped with 10m fibre was set at 42.206km to simulate the disturbance generated by acoustic wave.

To simplify the principle analysis, only two microstructures are taken into consideration, such as M_1 and M_2 given in Fig. 1 (b). Assuming the interval between adjacent microstructures is L. Due to the round trip, the reflected light from M_2 will be delayed by $2L$ compared to the one from M_1. Dual probe pulse is injected into the sensing fibre, which are separated with $2L$ in spatial domain. The dual pulse is originated from the same laser with angular frequency of ω_0, which are then frequency shifted by ω_1 and ω_2, respectively. Thus, at the time of t_1, $pulse_1$ arrives at M_1 and would be reflected. The electric field of reflected light E_{R1} can be written as:

$$E_{R1} = E_1 \cos\left[(\omega_0 + \omega_1)t + \varphi_0\right] \tag{1}$$

Where, E_1 is the amplitude of the reflected light from M_1, φ_0 is the initial phase. When the dual pulse propagating forward, $pulse_2$ will arrive at M_2 at the time of t_2 and would be reflected as well. At this point, E_{R1} arrives at M_2 and interferes with E_{R2}. The acoustic field could induce fibre length variation ΔL to the sensing fibre, thus creating phase change $\Delta\varphi$ between the reflected light waves from adjacent microstructures. Therefore, at t_2, the electric field of reflected lights generated by M_1 and M_2 can be written as:

$$E'_{R1} = E_1 \cos\left[(\omega_0 + \omega_1)t + \varphi_0 + \frac{4\pi n}{\lambda}(L + \Delta L)\right] \tag{2}$$

$$E_{R2} = E_2 \cos\left[(\omega_0 + \omega_2)t + \varphi_0\right] \tag{3}$$

The AC component of the photocurrent generated by the interference signal can be expressed as:

$$I(t) \propto 2E_1 E_2 \cos\left[(\omega_1 - \omega_2)t + \frac{4\pi n}{\lambda}L + \frac{4\pi n}{\lambda}\Delta L\right] = 2E_1 E_2 \cos\left[\omega_{IF}t + \varphi_{12} + \Delta\varphi\right] \tag{4}$$

The frequency of this beating signal is ω_{IF}, which is the difference between ω_1 and ω_2. φ_{12} is the initial phase difference between the two reflections. The relationship between ΔL and $\Delta\varphi$ can be written as:

$$\Delta\varphi = \frac{4\pi n}{\lambda}\Delta L \tag{5}$$

After phase demodulation, we can derive $\Delta\varphi$, and the corresponding fibre length variation ΔL can be obtained linearly according to Eq. (5).

3. Results and Discussion

In the experiment, the microstructures were realized with on-line manufactured Ultra Weak Fibre Bragg Grating (UWFBG) of 0.01% (-40dB) reflectivity. The interval between adjacent UWFBGs was 10m. The pulse width was 80ns to cover a region that was narrower than the interval of adjacent UWFBGs. The amplitude profile of obtained beating signal is shown in Fig.2 (a). Since Raman amplifying was induced, the magnitude of RBS was getting stronger at first along the fibre and reached its maximal around 15km. Then the signal slowly decreased all the way to the UWFBG region. As shown in Fig.2 (b), the reflected waves from UWFBGs region within the red dash line, were much stronger light waves than the RBS, which makes it possible to reconstruct the acoustic field even at the rear end of the sensing fibre with high SNR. The reflection from a given UWFBG could be distinguished from its nearby reflections, thus the interaction between adjacent UWFBGs could be analysed one by one clearly.

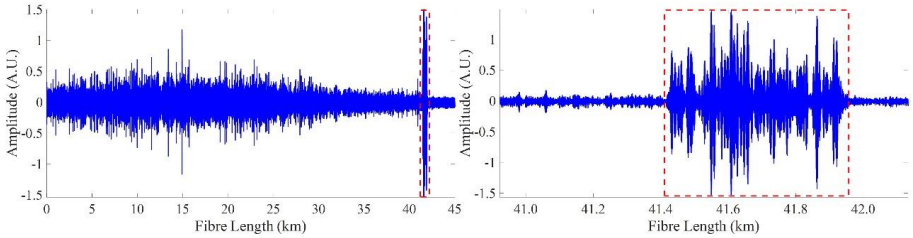

(a) (b)

Fig. 2 The obtained beating signal. (a) The entire amplitude profile of beating signal. (b) The zoomed amplitude profile near the UWFBGs region.

To evaluate the performance of the proposed system, a sinusoidal signal of 50Hz was applied on PZT to create periodical vibration. The voltage of the driving signal was 5V. The reconstructed acoustic signal in both time and frequency domains are given in Fig.3, which is of high fidelity. No obvious high order harmonics of the vibration signal were observed. A SNR of 36dB could be obtained between the peak value of vibration signal and far end noise floor as shown in Fig.3 (b).

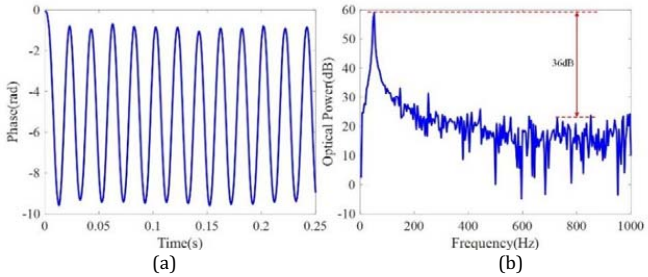

(a) (b)

Fig.3 The reconstructed signal (a) The time domain (b) The frequency domain

To verify the linear response property of the proposed system, the voltage applied on the PZT was swept from 0.5V to 10V while its frequency was fixed at 50Hz. Fig. 4(a) exhibits the waveform of the reconstructed acoustic signal at PZT after signal conditioning under different magnitudes. The reconstructed acoustic signal remained the shape of sinusoidal wave without distortion as the stretching of PZT was increased. In Fig. 4(b), the blue points were the measured amplitude of vibrations induced by PZT and the red dash line was the fitting result. The R-square of the fitting line was 0.99881, which confirmed a high level of linearity. Experiment has been made to further investigate the frequency response range of the proposed system. The repetition period of pulse was 500us, corresponding to the highest detectable frequency of 1 kHz according to the Nyquist rule of sampling. We tuned the frequency of the driving signal applied on PZT while its amplitude was fixed at 1V. For each frequency point, 500 consecutive traces were recorded for Fast Fourier

Transform (FFT). Fig. 4(c) shows the power spectrums obtained under different frequency points. The peak values were nearly of the same level all through the range from 8Hz to 1kHz.

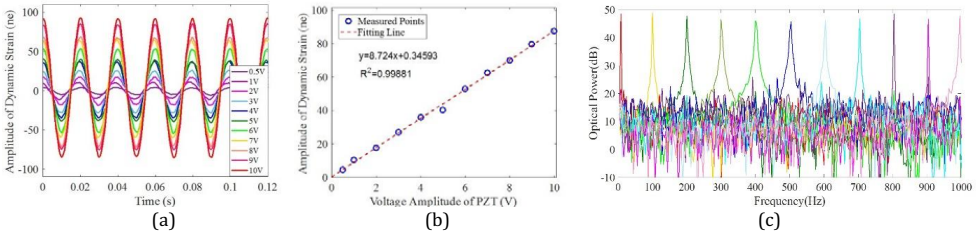

(a) (b) (c)

Fig.4 The amplitude of vibration changes as voltage of PZT3. (a) Detected vibrations of different voltages at PZT3. (b) Amplitude of vibration V.S. different PZT voltages at 50Hz and its fitting line. (c) Frequency response band of the proposed system

The proposed system presents an innovative view of the usage of microstructures in the enhancement of a DAS system. Taking advantage of the interaction process between nearby microstructures, the distribution of acoustic field along the sensing fibre could be fully captured. The reconstruction of acoustic field is equivalent to the measurement of optical path variation induced by external disturbance, and finally converted into the observation on phase change of reflected light waves from adjacent microstructures all along the sensing fibre. By comparing the signals before and after UWFBGs as shown in Fig. 2, the SNR enhancement was approximately 18dB. That means the sensing fibre length would be improved by nearly 45km considering a round trip attention ratio of 0.4dB/km. The spatial resolution of the proposed system was mainly determined by the interval between adjacent UWFBGs. Higher spatial resolution could be obtained if the interval between UWFBGs is reduced. Purely distributed sensing along the optical fibre was achieved even with discretely implanted microstructures for the proposed system, which offers a dependable option for long range distributed acoustic sensor enhancement.

4. Conclusion

We present an enhanced DAS system based on the interactions between microstructures implanted into the optical sensing fibre. The acoustic field could be reconstructed with high fidelity even at the rear end of 42.2km long sensing fibre. The experimental results have shown that the proposed sensing system has a linear intensity response of R^2=0.9988, while its frequency response band ranges from 8Hz to 1 kHz.

References

[1] X. W. Ye, Y. H. Su,J. P. Han 2014 *The Scientific World Journal* **2014** 652329
[2] H. N. Li, D. S. Li,G. B. Song 2008 *Steel Construction* **26** 1647-1657
[3] L. Deng,C. S. Cai 2007 *Structural Engineering & Mechanics* **25** 577-596
[4] J. C. Juarez, E. W. Maier, K. N. Choi,H. F. Taylor 2005 *Journal of Lightwave Technology* **23** 2081-2087
[5] Q. He, T. Zhu, W. Huang,X. Bao 2014 *International Conference on Optical Fibre Sensors* 915761-915761-4
[6] F. Peng etal 2014 *Optics Express* **22** 13804
[7] F. Peng, N. Duan, Y. J. Rao,J. Li 2014 *Photonics Technology Letters IEEE* **26** 2055-2057
[8] Z. Zhang,X. Bao 2008 *Journal of Lightwave Technology* **26** 832-838
[9] Z. Sha etal *IEEE Photonics Technology Letters* 1-1
[10] X. Tian etal 2016 *Proceedings of the Spie* **158**
[11] H. F. Martins etal 2013 *Optics Letters* **38** 872
[12] Z. Wang etal 2014 *Ofs2014 International Conference on Optical Fibre Sensors*
[13] J. Li etal 2014 *Society of Photo-Optical Instrumentation Engineers* 91575Z-91575Z-4
[14] Z. N. Wang etal 2014 *Optics Letters* **39** 4313
[15] H. F. Martins etal 2014 *Journal of Lightwave Technology* **32** 1510-1518
[16] C. Wang etal 2015 *Optics Express* **23** 29038-46
[17] F. Zhu etal 2015 *Journal of Lightwave Technology* **33** 4775-4780
[18] X. Wang etal 2015 *IEEE Photonics Journal* **7** 1-11